QUARTERLY OF APPLIED MATHEMATICS
VOLUME XLIV, NUMBER 4
JANUARY 1987, PAGES 779-792

ASYMPTOTIC EXPANSIONS IN NONLINEAR ROTORDYNAMICS*

BY

WILLIAM B. DAY [1]

Auburn University

Abstract. This paper is an examination of special nonlinearities of the Jeffcott equations in rotordynamics. The immediate application of this analysis is directed toward understanding the excessive vibrations recorded in the LOX pump of the SSME during hot-firing ground testing.

Deadband, side force, and rubbing are three possible sources of inducing nonlinearity in the Jeffcott equations. The present analysis initially reduces these problems to the same mathematical description. A special frequency, named the nonlinear natural frequency, is defined and used to develop the solutions of the nonlinear Jeffcott equations as singular asympotic expansions. This nonlinear natural frequency, which is the ratio of the cross-stiffness and the damping, plays a major role in determining response frequencies.

Numerical solutions are included for comparison with the analysis. Also, nonlinear frequency-response tables are made for a typical range of values.

1. Introduction. Vibrations are inherent in rotating machinery. Mathematical explanations of vibrations began with Jeffcott's description of the shaft's natural frequency of lateral vibration [6]. Unfortunately, Jeffcott's linear model cannot account for all frequencies that have been observed experimentally. In particular, destructive vibrations have occurred in hot-firing ground testing of the liquid oxygen pump of the space shuttle's main engine with no clue to these vibrations' origins being offered by the linear model. Specifically, examination of the power spectral density (PSD) plots reveals unaccountable frequencies. Consequently, numerous investigations have been undertaken to study such rotors and to provide descriptions of the solutions of the two coupled, second-order differential equations which describe the motion of the rotor's center of mass.

Following the early work in rotordynamics by Yamamoto [9], one introduces a nonlinearity to the Jeffcott equations by including the effect of bearing clearance or deadband. In the pump, this deadband refers to the load carriers (ball bearings) and physically describes the clearance between the outer race of the bearing and the support

* Received September 17, 1985.
[1] This work was supported by NASA George C. Marshall Space Flight Center, under contract NAS8-35992.

housing. The work of Yamamoto did not include cross-stiffness, but a straightforward derivation with this modification is easily obtained. A more limiting gap in his work is the assumption that the response is simply a perturbation of the forcing function. This is tantamount to assuming that one always has the graph of a circle as the solution.

It is shown in this paper that this generally is not the case. Both empirical results by Childs [2, 3] and Gupta et al. [5] and numerical solutions have been helpful in understanding the rotor's motion for the nonlinear problem. This paper extends the earlier work by using analytic expressions obtained from singular asymptotic expansions (method of multiple scales) to quantize the solution.

Section 2 is the formal mathematical development of analytic solutions. This section includes the discovery of the nonlinear natural frequency and proceeds to incorporate it in an asymptotic expansion of the solution. Herein also lies an explanation of why one expects the rotor's motion to be either a circle or an annulus.

Section 3 contains numerical examples which verify the theoretical expansions. Typical frequency-response descriptions are also included in this part.

Section 4 concludes with a summary of the paper's applications and directions for future studies.

2. General theory.

2.1. *Nondimensionalization.* The linear Jeffcott equations which describe the displacement of the rotor center from its equilibrium position in the inertial, Cartesian coordinate system (y, z) are these:

$$m\ddot{y} = -C_s\dot{y} - K_s y - Q_s z + mu\omega^2 \cos \omega t, \tag{1}$$

$$m\ddot{z} = -C_s\dot{z} + Q_s y - K_s z + mu\omega^2 \sin \omega t, \tag{2}$$

where the shaft of the rotor lies along the x-axis and

m = mass,

C_s = seal damping,

K_s = seal stiffness,

Q_s = cross-coupling stiffness of seal,

u = displacement of the shaft center of mass from the geometric center,

ω = angular velocity of the shaft (rad/sec).

For the model to include bearing forces which hold the rotor in position, one adds the terms

$$-K_b\left(y - y\delta/\sqrt{y^2 + z^2}\right) + \mu K_b\left(z - z\delta/\sqrt{y^2 + z^2}\right)$$

and

$$-\mu K_b\left(y - y\delta/\sqrt{y^2 + z^2}\right) - K_b\left(z - z\delta/\sqrt{y^2 + z^2}\right),$$

respectively, to right-hand sides of Eqs. (1) and (2). Here,

K_b = bearing stiffness,

δ = clearance or deadband between housing and bearing,

μ = coefficient of friction between housing and bearing.

These bearing forces occur only when $\sqrt{y^2 + z^2} > \delta$; otherwise, they are zero. Since μ is nondimensional and typically small, one may regard it as zero without affecting the qualitative results.

Equations (1) and (2) then become

$$\ddot{y} + (C_s/m)\dot{y} + (1/m)\left[K_s + K_b(1 - \delta/r)\right] y + (Q_s/m) z = u\omega^2 \cos \omega t, \tag{3}$$

$$\ddot{z} + (C_s/m)\dot{z} - (Q_s/m) y + (1/m)\left[K_s + K_b(1 - \delta/r)\right] z = u\omega^2 \sin \omega t \tag{4}$$

when $r = \sqrt{y^2 + z^2} > \delta$; otherwise, $K_b = 0$. Equations (3) and (4) can be put in nondimensional form using a displacement g and a frequency σ. One pair of candidates for g and σ would be $g = \delta$, the deadband size, and $\sigma^2 = \omega_0^2 = K_s + K_b$, the natural frequency of the corresponding linear problem ($\delta = 0$). Thus, using $Y = y/g$, $Z = z/g$, and $\tau = \sigma t$, the dimensionless equations are these:

$$Y'' + CY' + \left[A + \kappa(1 - \Delta/R)\right] Y + BZ = E\phi^2 \cos \phi\tau, \tag{5}$$

$$Z'' + CZ' - BY + \left[A + \kappa(1 - \Delta/R)\right] Z = E\phi^2 \sin \phi\tau, \tag{6}$$

where prime denotes differentiation with respect to τ and $C = C_s/m/\sigma$, $A = K_s/m/\sigma^2$, $k = K_b/m/\sigma^2$, $B = Q_s/m/\sigma^2$, $\Delta = \delta/g$, $R = r/g$, $E = u/g$, and $\phi = \omega/\sigma$.

Equations (5) and (6) can be reduced to the following single equation by defining $W = Y + iZ$:

$$W'' + CW' + \{A + k(1 - \Delta/|W|) - iB\} W = E\phi^2 \exp(i\phi\tau). \tag{7}$$

Furthermore, the polar form of Eqs. (5) and (6) is

$$R'' + CR' + \left[A + \kappa(1 - \Delta/R) - (\Theta')^2\right] R = E\Phi^2 \cos(\phi\tau - \Theta), \tag{8}$$

$$R\Theta'' + (2R' + CR)\Theta' = R\left[B - \mu k(1 - \Delta/R)\right] + E\phi^2 \sin(\phi\tau - \Theta), \tag{9}$$

where $R = (Y^2 + Z^2)^{1/2}$ and $\Theta = \text{Arctan}(Z/Y)$.

The nondimensional Jeffcott equations with deadband and mass imbalance are easily solved numerically using a fourth-order Runge-Kutta algorithm. If these solutions are then plotted and analyzed in a power spectral density (PSD) investigation, the resulting graphs provide a direction for initial, analytic descriptions. To this end, consider the following special case:

$$\begin{aligned} m &= 1, & u &= 1.5\delta, \\ C &= 240, & Q &= 200{,}000, \\ K_s &= 0, & \delta &= 0.0000285, \\ K_b &= 1{,}350{,}000, & \omega &= 500 \text{ Hz}. \end{aligned}$$

Therefore, with $\omega_0 = (1{,}305{,}000)^{1/2}$ and $\delta = 0.0000285$ as the nondimensionalizing parameters, the Jeffcott equations become

$$Y'' + (C_s/\omega_0) Y' + (1 - 1/R) Y + \left(Q_s/\omega_0^2\right) Z = 1.5(\omega/\omega_0)^2 \cos(\omega/\omega_0)\tau,$$

$$Z'' + (C_s/\omega_0) Z' - \left(Q_s/\omega_0^2\right) Y + (1 - 1/R) Z = 1.5(\omega/\omega_0)^2 \sin(\omega/\omega_0)\tau,$$

where $\tau = \omega_0 t$ and $R = (Y^2 + Z^2)^{1/2}/\delta$. Fig. 1 shows the motion for this case. The motion has become periodic for the time interval ($0.5 \leqslant t \leqslant 1$) shown. The graph of t vs. $r = \delta R$, given in Fig. 2, suggests that r has the form

$$r = 0.71 + 0.39 \cos 720\pi t = a_0 + a_1 \cos \gamma\tau.$$

It is this form that leads one to consider approximating the Jeffcott equations with

$$Y'' + CY' + (1 - 1/(a_0 + a_1 \cos \gamma\tau))Y + BZ = 1.5\phi^2 \cos \phi\tau,$$

$$Z'' + CZ' - BY + (1 - 1/(a_0 + a_1 \cos \gamma\tau))Z = 1.5\phi^2 \sin \phi\tau.$$

Examination of the PSD of R shows that R is actually an infinite sum:

$$R = \sum_{k=0}^{\infty} a_k \cos k\gamma\tau,$$

with $a_0 + a_1 \cos \gamma\tau$ the dominant terms. The other coefficients decrease exponentially to zero as $k \to \infty$. At this point, one may proceed to write the expansion for $1/R$ in the form $1 + E \cos \gamma\tau + O(E^2)$ and to expand the displacements Y and Z as asymptotic series in E. This leads to solutions that "look" correct, but then they should. After all, we have obtained the solutions from approximating equations that used the solutions (in R) a priori.

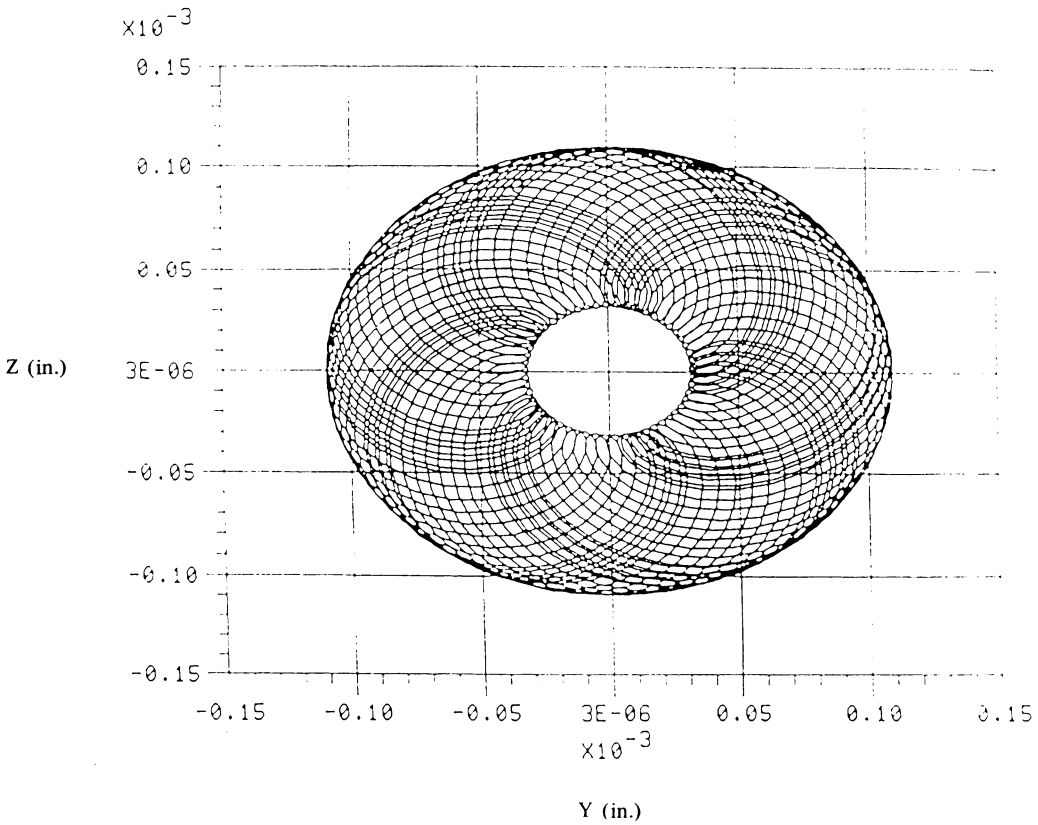

FIG. 1.

Guided by these numerical results, we begin again to examine the differential equations; however, this time we investigate the source of the nonlinear (the $1/R$ term) natural (homogeneous equation) frequency.

2.2. *Nonlinear natural frequency.* Consider the dimensional, homogeneous ($E = 0$) equation corresponding to Eq. (7):

$$\ddot{w} + (C_s/m)\dot{w} + (1/m)\{[K_s + K_b(1 - \delta/r) - iQ_s]\}w = 0, \tag{7'}$$

where $w = y + iz$. If this equation were also linear ($\delta = 0$), then exponentially growing or decaying solutions would generally result for a given set of system parameters. In the special case that $(Q_s/C_s)^2 = K_s + K_b$, a sinusoidal solution is obtained with frequency $\beta_0 = Q_s/C_s$. To see this, consider the characteristic equation for $w = \exp(pt)$:

$$p^2 + C_s p + [K_s + K_b - iQ_s] = 0$$

$$P = -C_s/2 \pm \{C_s^2/4 - K_s - K_b + iQ_s\}^{1/2} = -C_s/2 \pm \{C_s^2/4 - (Q_s/C_s) + iQ_s\}^{1/2}$$

$$P = -C_s/2 \pm i\{iC_s/2 - Q_s/C_s\} = -C_s - iQ_s/C_s, \qquad iQ_s/C_s.$$

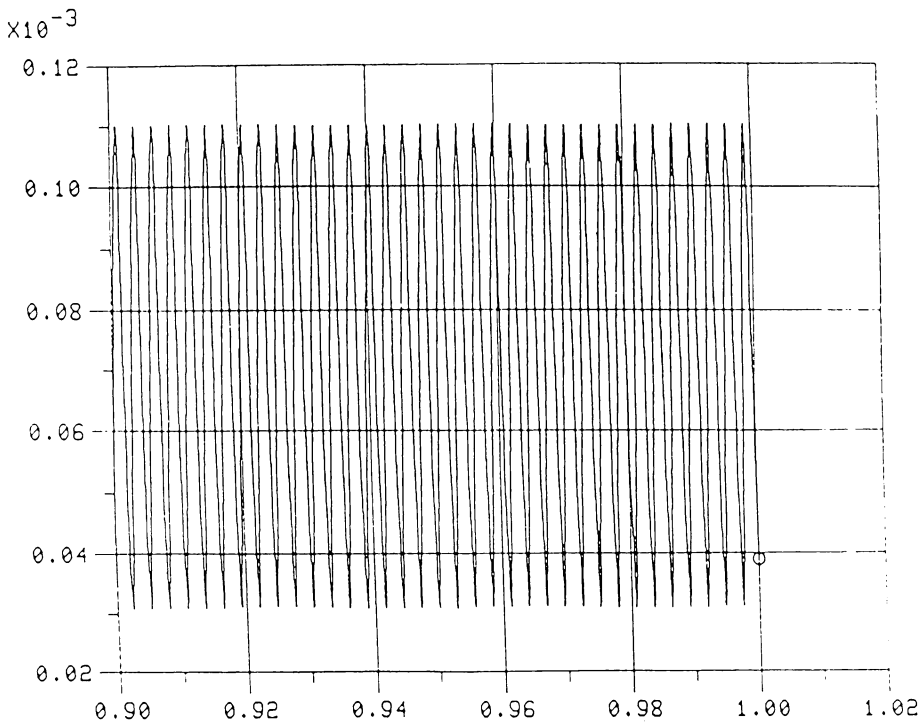

FIG. 2.

In the nonlinear, homogeneous problem, K_b is replaced by $K_b(1 - \delta/r)$; hence, if r is a constant, then there is a wide spectrum of r for which $(Q_s/C_s)^2$ may be $K_s + K_b(1 - \delta/r)$; i.e., if

$$K_s < (Q_s/C_s)^2 \leqslant K_s + K_b, \tag{10}$$

then there is a constant value of r (with $r > \delta$) for which $(Q_s/C_s)^2 = K_s + K_b(1 - \delta/r)$. This value of r is denoted by a and the corresponding frequency by $\beta_0 = Q_s/C_s$. This frequency is labeled the nonlinear natural frequency. Thus, whenever inequality (10) is satisfied, Eqs. (3) and (4) with $u = 0$ have steady-state solutions $y = a\cos(\beta_0 t)$ and $z = a\sin(\beta_0 t)$.

Notice that $\beta_0 = Q_s/C_s \leqslant (K_s + K_b)^{1/2} = \omega_0$, the dimensional natural frequency of the linear system. Thus, in considering the general nonhomogeneous problem, it is necessary to be aware of these three-dimensional frequencies:

$$\beta_0 = \text{the nonlinear natural frequency,}$$
$$\omega_0 = \text{the natural frequency, and}$$
$$\omega = \text{the driving frequency.}$$

Either β_0 or ω_0 is an appropriate choice for σ, the nondimensionalizing frequency. Correspondingly, one would select either a (with β_0) or δ (with ω_0) as the base displacement s.

One final rearrangement of Eq. (7) is made here to emphasize the nonlinear natural frequency:

$$W'' + CW' + \kappa W = f(W) + E\phi^2 \exp(i\phi\tau), \tag{11}$$

where $\kappa = A + k(1 - \Delta/a) - iB$ and $f(W) = k\Delta[1/|W| - 1/a]W$.

2.3. *Equivalent problems.* In this subsection the forcing function is assumed to have the form $F(\omega)\exp(i\omega t)$, where $F(\omega) \geqslant 0$ (or equivalently $F(\omega) \leqslant 0$) and F is single-valued for $\omega \geqslant 0$. The following are special cases of physical interest:

a. *Mass imbalance.* As discussed above, $F(\omega) = u\omega^2$ for a mass u.

b. *Side force.* This force may be introduced into the Jeffcott Eqs. (1) and (2) as constant replacements for the mass imbalance. In such cases, Eq. (7) becomes

$$W'' + CW' + \{A + k(1 - \Delta/|W|)iB\}W = u\omega^2/\delta g^2 = \text{constant}.$$

Thus, a side force is the special case $F(\omega) = \text{constant}$ and $\omega = 0$.

c. *Rubbing.* Rubbing contact between a rotor and its housing produces a Coulomb damping force. This force would modify the original Jeffcott equations by the addition of the terms:

$$K_{st}(1 - \delta/r)y - \mu K_{st}(1 - \delta/r)z + K_{st}(1 - \delta/r)G$$

and

$$\mu K_{st}(1 - \delta/r)y + K_{st}(1 - \delta/r)z + \delta K_{st}(1 - \delta/r)G,$$

respectively, to the right-hand sides of Eqs. (1) and (2). Here, G = constant = stator offset in the y-direction, K_{st} = stator stiffness, and μ = coefficient of friction, which may not be small. As before, these forces would be included only when $r = (y^2 + z^2)^{1/2} > \delta$. On

replacing $y - G$ by y, Eq. (7) (and correspondingly its equivalent forms) again occurs but with these modifications:

1. $i[-B]$ is replaced by

$$i\left[-B + \mu\left(K_{st}/g^2\right)(1 - \Delta/R)\right];$$

2. the forcing function $E\phi^2 \exp(i\phi\tau)$ is replaced by

$$E\phi^2 \exp(i\phi\tau) + \left(-\omega_0^2/g^2\right)(G/\delta).$$

If the mass imbalance term is omitted, then one may regard the deadband with side force problem and the rubbing problem as equivalent. Notice that the range of values of the parameters for these two problems may not be the same since the rubbing problem includes the possibly nonnegligible term $\mu(K_{st}/g^2)(1 - \Delta/r)$.

2.4. *Method of multiple scales.* First, one may relate Eq. (7) to Mathieu's or Hill's equation (see Cesari [1]) except that the periodic coefficient $(1/|W|)$ is not independent of W. Another approach is to consider autonomous, nonlinear systems, which have been extensively discussed in the literature (see Kubicek and Marek [7]); however, a transformation to an autonomous system yields no new insight.

The discontinuous derivative in the stiffness, $K_s + K_b(1 - \delta/r)$, does not affect our solution within the parameters' allowed value ranges. Similar discontinuities for homogeneous, nonlinear problems have been explored by Dinca and Teodosiu [4]; however, it is the interaction of the homogeneous solution and the term resulting from the forcing function that causes the interesting behavior in this problem.

Straightforward asymptotic expansions, which lead to the zero-order approximation $W_0 = M\exp(i\beta_0\tau) + N\exp(i\beta_0\tau)$, are not general enough for this problem. We must allow M and β_0 to become functions of time. Either the method of averaging or the method of multiple scales, as described in Nayfeh [8], is appropriate.

Instead of one time scale τ, assume the problem depends on many time scales:

$$T_0 = \tau,\ T_1 = \varepsilon\tau,\ T_2 = \varepsilon^2\tau, \ldots.$$

Henceforth, only T_0 and T_1 are used. Let

$$W(\tau) = W(T_0, T_1) = W_0(T_0, T_1) + \varepsilon W_1(T_0, T_1) + \cdots.$$

Equation (11) becomes a partial differential equation since

$$d/d\tau = (\partial/\partial T_0)(dT_0/d\tau) + (\partial/\partial T_1)(dT_1/d\tau) = D_0 + \varepsilon D_1$$

and

$$\left(d^2/d\tau^2\right) = \left(D_0 + \varepsilon D_1\right)^2.$$

Thus, one finds

$$\left(D_0 + \varepsilon D_1\right)^2(W_0 + \varepsilon W_1 + \cdots) + C(D_0 + \varepsilon D_1)(W_0 + \varepsilon W_1 + \cdots) + \kappa(W_0 + \varepsilon W_1 + \cdots)$$
$$= \varepsilon f(W_0 + \varepsilon W_1 + \cdots) + E\phi^2 \exp(i\phi T_0). \tag{12}$$

Equating like powers of ε yields

$$\varepsilon^0: \qquad D_0^2 W_0 + CD_0 W_0 + \kappa W_0 = E\phi^2 \exp(i\phi T_0). \tag{13}$$

This is a linear problem with a steady-state solution

$$W_0 = M\exp(i\beta_0 T_0) + N\exp(i\phi T_0),$$

where $N = E\phi^2/(-\phi^2 + iC\phi + \kappa)$ and $M = M(T_1)$. To determine M one must examine the ε-order problem and choose M to eliminate secular terms:

$$\varepsilon^1: \qquad D_0^2 W_1 + CW_1 + \kappa W_1 = -2D_0 D_1 W_0 - CD_1 W_0 + f(W_0).$$

With $L = k\Delta/\varepsilon$, the right-hand side of the last equation becomes

$$-2i\beta_0 M'\exp(i\beta_0 T_0) - CM'\exp(i\beta_0 T_0) + L(1/|W_0| - 1)\left[M\exp(i\beta_0 T_0) + N\exp(i\phi T_0)\right],$$

where $|W_0| = \{|M|^2 + |N|^2 + \bar{M}N\exp[i(\phi - \beta_0)T_0] + M\bar{N}\exp[i(\beta_0 - \phi)T_0]\}^{1/2}$. To avoid secular terms one requires that the collective coefficient of $\exp(i\beta_0 T_0)$ be zero. Although an analytic solution of the differential equation for $M(T_1)$ has not been found, one can qualitatively assess M based on a similar problem (van der Pol's equation) and specific numerical results (presented in the next section).

Since $M(T_1)$ is complex, it may be written as $M(T_1) = \rho(T_1)\exp[i\hat{\beta}(T_1)]$. Thus,

$$W_0 = \rho(t_1)\exp\left[i\beta_0 T_0 + i\hat{\beta}(T_1)\right] + N\exp(i\phi T_0),$$

or, assuming $\hat{\beta}(T_1)$ is analytic near $t = 0$,

$$W_0 = \rho(T_1)\exp\left[i(\beta_0 + \varepsilon\beta_1)\tau + \cdots\right] + N\exp(i\phi\tau).$$

Thus the fundamental frequency of the nonlinear problem is not β_0 but $\beta = \beta_0 + \varepsilon\beta_1 + \cdots$; however, β must reduce to β_0 when $E\phi^2 = 0$. This frequency shift can account for the phenomenon of "tracking" that has been observed experimentally [3]. Similarly, the frequency $\gamma = \phi - \beta_0$ that appears in the expression for $|W_0|$ should be $\gamma = \phi - \beta$. Then $1/|W_0|$ shows all frequencies $n\gamma$, and $W_0/|W_0|$ shows all frequencies $n\gamma \pm \beta$ for $n = 0, 1, \ldots$. This suggests that M has a complex Fourier series of the form

$$\sum_{n=-\infty}^{\infty} s_n \exp(in\gamma T_1).$$

Another factor of M must also be included since numerical examples show that $M \equiv 0$ if $E\phi^2$ is greater than some fixed value. This is similar to the behavior of the van der Pol oscillator (see [8]). Thus, one may speculate that M has a factor of the form $F = 1/[1 + \exp(-\eta T_1)]$ where $\eta = \eta(E\phi^2)$. This would imply that $F \to 1$ as $\tau \to \infty$ when $\eta > 0$ and $F \to 0$ as $\tau \to \infty$ when $\eta < 0$. Thus, M looks like

$$1/\left[1 + \exp(-\eta T_1)\right] \sum_{n=-\infty}^{\infty} s_n \exp(in\gamma T_1).$$

PSD plots of R show only frequencies of $n\gamma$, while plots of Y show frequencies of ϕ and $n\gamma \pm \beta$.

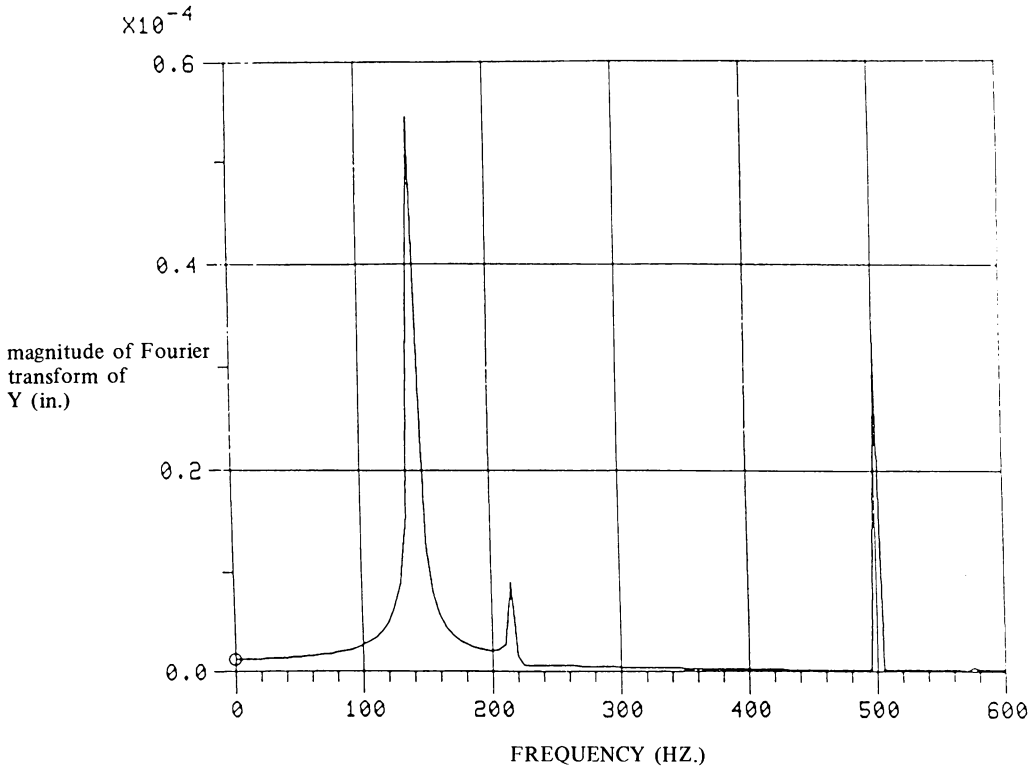

FIG. 3.

3. Examples. This section contains two numerical examples of the theory presented in Sec. 2. The first example shows how the solution changes for a fixed forcing frequency but increasing forcing magnitudes. Example 2 is a frequency-response illustration of variations in the forcing frequency and corresponding responses.

Example 1. In this example the system constants used are these: $\mu = 0$, $m = 1$ lb-s^2/in., $C = 240$ lb-s/in., $K_s = 0$, $K_b = 1{,}305{,}000$ lb/in., $Q_s = 200{,}000$ lb/in., $\delta = 0.0000285$ in., and $\omega = 500$ Hz $= 1{,}000\,\pi$ rad/s. Thus, $\beta_0 = 833.33$ rad/s and $a = 0.000060915$ in. The system is made nondimensional using a for the g-displacement and β for the σ-frequency. With these choices, the constants of this equation

$$W'' + CW + [k(1 - \Delta/|W|) - iB]W = E\phi^2 \exp(i\phi\tau)$$

have these values: $C = 0.288$, $k = 1.8792$, $\Delta = 0.467865$, $B = 0.288$, and $\phi = 6\pi/5$.

Figures 4 and 5 show changes in the solution Y vs. Z as E assumes the values $100n/(1{,}000\pi)^2\ a$ for $n = 0, 1, \ldots, 7$. The graphs are plotted for $0.2 < t \leqslant 0.5$. The initial circle (for $E = 0$) opens into an annular region, which becomes larger and thicker as E increases until a (transition) value of E occurs and the coefficient of $\exp(i\beta\tau)$ becomes zero. Thus, $W = N\exp(i\phi\tau)$, a circle of radius $|N|$. As E increases beyond this transition

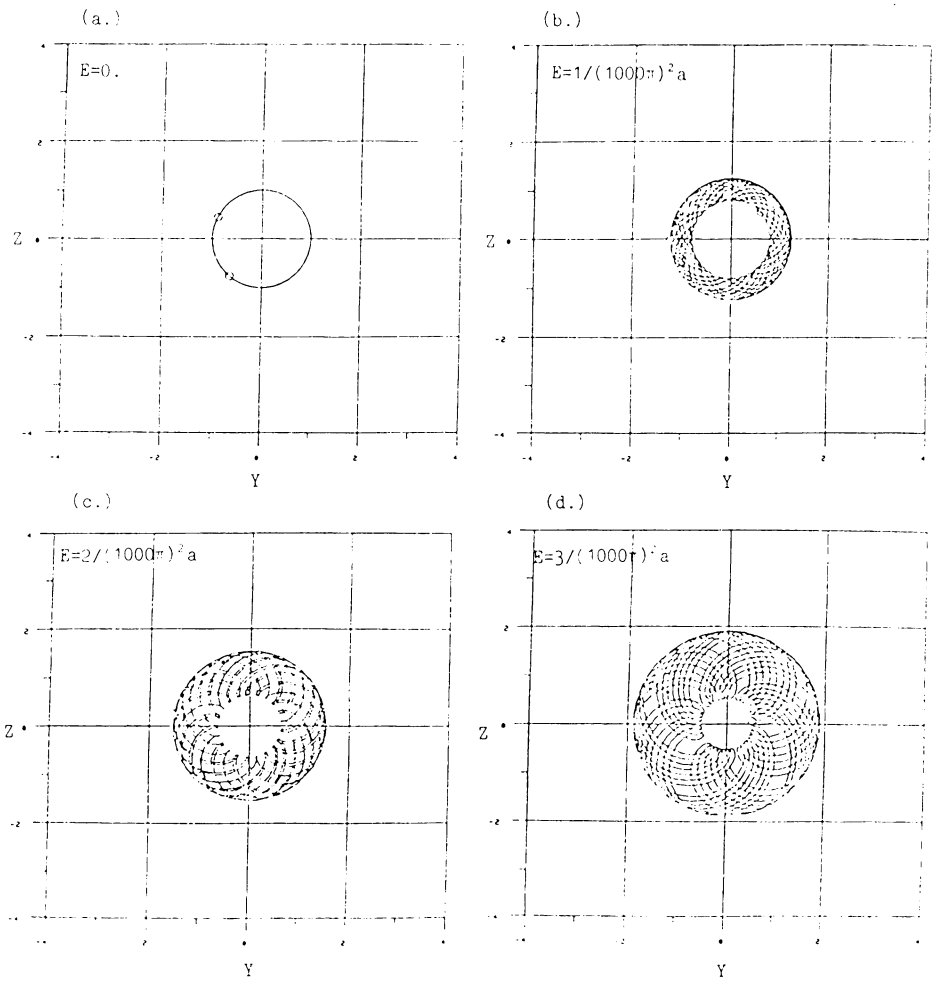

FIG. 4.

value, the solution remains a circle (Fig. 5d) with radius $|N| = |E\phi^2/(-\phi^2 + iC\phi + k(1 - \Delta/|N|) - iB)|$.

Example 2. As described above, one expects either a circle or an annulus at each fixed forcing frequency ϕ. Furthermore, near resonance one always finds a circle since the characteristic frequency is entrained by the forcing frequency. Considering that the forcing function is a continuous function of this frequency ϕ, it follows that the solution is a circle or an annulus over an interval of the ϕ-axis, and that the number of transitions between the two shapes is finite over a bounded portion of the positive ϕ-axis.

Tables I, II, and III illustrate these results for the problem with these parameter values:

$$C_S s = 240/\omega_0, \qquad \delta = 0.0000285,$$
$$Q_s = 200{,}000/\omega_0^2, \quad E = 0.5, 1.0, \text{ or } 1.5,$$
$$K_s = 0, \qquad K_b = 1{,}305{,}000 = \omega_0^2.$$

Tables I, II, and III are for the three cases $E = 0.5$, 1.0, and 1.5, respectively. In all three cases, ω_0 is used as the nondimensionalizing frequency. Each of the three tables describes the response curve by listing the radius of circles or the inner and outer radii for annuli. Furthermore, the frequency $\gamma = |\beta - \omega|$ is given for annuli. The values listed for ϕ are every 0.1 except when

1. more refinement is required to bound better the transition point, and
2. less refinement is needed because of small variation in the response at different frequencies.

Particular attention should be paid to Table III since it shows three different regions in which the circle appears as the solution. The first two tables contain only one such region.

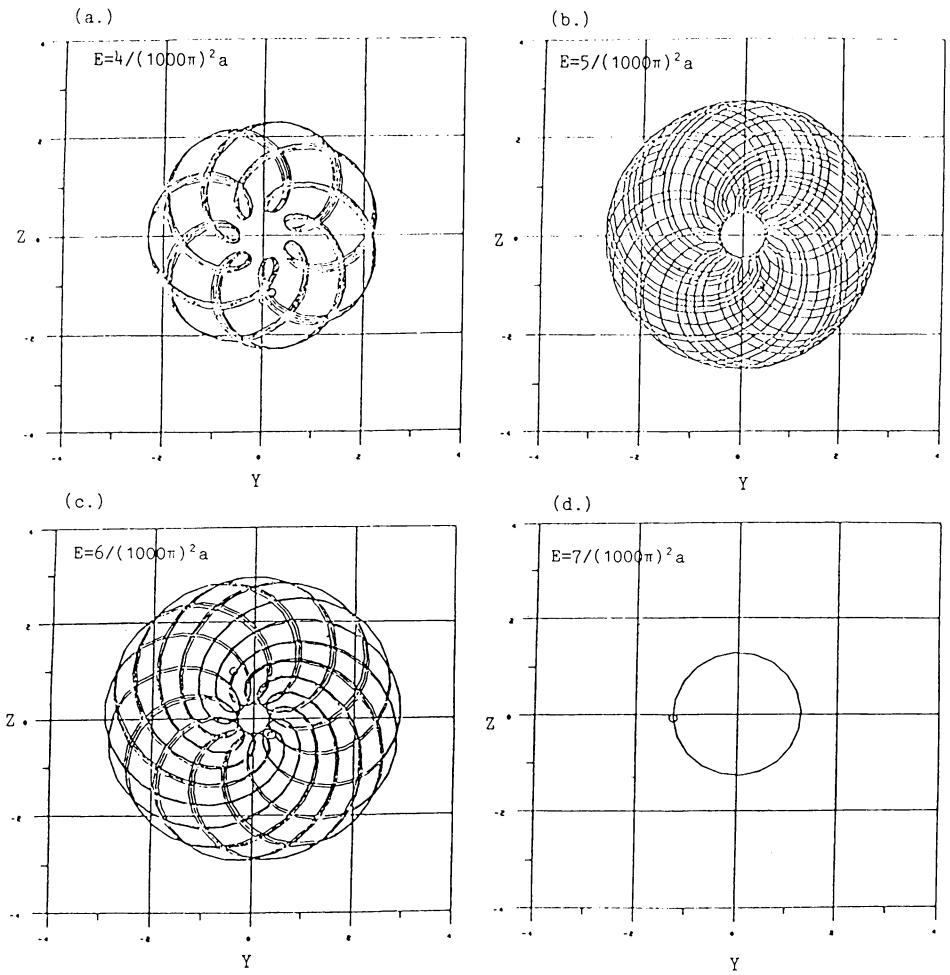

FIG. 5.

TABLE I
$E = 0.5$

ϕ	Shape (Circle/Annulus)	Radius (Radii)	γ(Hz.)
0.0	C	2.137	—
0.1	A	2.130–2.145	115
0.2	A	2.105–2.169	97
0.4	A	1.959–2.305	61
0.5	A	1.747–2.470	41
0.53	A	1.618–2.549	34
0.54	C	1.597	–
0.6	C	1.833	–
0.7	C	2.441	–
0.8	C	3.656	–
0.9	C	6.954	–
0.92	C	8.249	–
0.93	A	1.212–4.018	13
1.0	A	1.369–3.230	40
1.2	A	1.551–2.858	81
1.4	A	1.643–2.822	118
1.6	A	1.648–2.748	154
1.8	A	1.694–2.633	190
2.0	A	1.804–2.679	222
2.2	A	1.939–2.830	263
2.4	A	1.993–3.162	294
2.6	A	1.632–3.125	333
2.8	A	1.533–2.864	370
3.0	A	1.528–2.769	410

TABLE II
$E = 1.0$

ϕ	Shape (Circle/Annulus)	Radius (Radii)	γ(Hz.)
0.0	C	2.137	–
0.2	A	2.073–2.201	98
0.4	A	1.767–2.463	60
0.41	A	1.737–2.486	58
0.42	C	1.398	–
0.5	C	1.650	–
0.6	C	2.118	–
0.8	C	4.548	–
0.9	C	9.174	–
0.97	C	18.524	–
0.99	C	10.436	–
1.0	A	0.872–2.033	12
1.2	A	1.003–4.194	68
1.4	A	1.145–3.972	96
1.6	A	1.431–3.839	145
1.8	A	1.151–3.283	185
2.0	A	1.341–3.296	222
2.2	A	1.598–3.499	256
2.4	A	1.871–3.932	286
2.6	A	1.732–4.456	322
2.8	A	1.062–3.745	357
3.0	A	0.981–3.390	400

TABLE III
$E = 1.5$

ϕ	Shape (Circle/Annulus)	Radius (Radii)	γ(Hz.)
0.0	*C*	2.137	–
0.2	*A*	2.040–2.230	96
0.3	*A*	1.885–2.371	78
0.35	*A*	1.755–2.476	68
0.36	*C*	1.364	–
0.4	*C*	1.449	–
0.6	*C*	2.398	–
0.8	*C*	5.427	–
0.9	*C*	11.269	–
0.98	*C*	27.247	–
0.99	*C*	25.102	–
1.0	*C*	19.448	–
1.2	*C*	2.585	–
1.38	*C*	2.028	–
1.39	*A*	0.357–4.628	99
1.4	*A*	0.529–4.832	100
1.6	*A*	0.837–4.660	139
1.77	*A*	0.359–3.832	172
1.78	*C*	1.717	–
1.8	*C*	1.709	–
1.91	*C*	1.676	–
1.92	*A*	0.100–3.121	195
2.0	*A*	0.496–3.282	217
2.2	*A*	1.062–4.076	250
2.4	*A*	1.496–4.564	286
2.6	*A*	1.692–5.341	312
2.8	*A*	0.222–3.987	359
2.81	*C*	1.565	–
2.9	*C*	1.560	–
3.0	*C*	1.555	–

4. Conclusions. This paper has shown how vibrations at frequencies which are unexplainable by linear theory can be expected in nonlinear Jeffcott models which consider deadband, side forces, or rubbing. These frequencies and their regions of stability are bounded by parameters of the differential equations. Although the asymptotic analysis is weak in quantizing exactly the frequencies and the corresponding magnitudes, there exist simple numerical methods which may be employed for the desired precision. The analysis, then, serves as a guide in locating nonlinear vibrations, which the numerical techniques then find accurately.

In studying the Jeffcott rotor with deadband or rubbing and sinusoidal forcing (including constant side force), one must consider these three frequencies: (a) the forcing frequency ω; (b) the natural frequency ω_0 of the associated linear problem (deadband = $\delta = 0$); and (c) the nonlinear natural frequency β_0. The frequency ω depends only on the forcing function; ω_0 depends only on the system parameters; β, with its base value β_0, depends on both the forcing function and the system parameters. For a specific set of equation parameters, one can find this nonlinear natural frequency β_0 as the ratio of cross-stiffness to damping.

For a given system and a nonzero, external, sinusoidal force, the $y - z$ response is either a circle at the forcing frequency or an annulus composed of the (major) frequencies ω and β as well as the (minor) harmonic frequencies $n(\omega - \beta) \pm \beta$ for positive integers n.

There are several unanswered questions. First, can one cast this problem as one in bifurcation theory. Second, it would also be nice to know, for a given set of parameters, the exact frequency values at which the response switches between circles and annuli. Based on similar results for the van der Pol oscillator, these transition points should exist as analytic expressions, thereby avoiding numerical iterations.

The asymmetric stiffness problem, which many reports have hypothesized as being the culprit of instability, is vastly more complex than the symmetric case. Preliminary Runge–Kutta solutions show not only that the circle/annulus plots become elliptic and occur with their axes rotated with respect to the y, z axes, but that there may be other shapes and many transition points to consider. These problems, however, greatly extend the model's mimicry of an observed rotor's behavior.

Finally, this paper is also limited to single forcing functions. Realistically, one must consider multiple forcing functions. Superposition will fail for the nonlinear problem, although it may be a first approximation.

Stability for all these problems remains the central focus. Even in the symmetric nonlinear problem with a single driver, it is still an open question of whether the response may move from an annulus to a circle (or vice versa) when it is perturbed.

References

[1] L. Cesari, *Asymptotic behavior and stability problems in ordinary differential equations*, Academic Press, 1963.

[2] D. W. Childs, *The Space Shuttle main engine high-pressure fuel turbopump rotordynamics instability problem*, Trans. ASME, J. Engrg. for Power, 48–57 (January 1978)

[3] D. W. Childs, *Rotordynamic characteristics of the HPOTP (high pressure oxygen turbopump) of the SSME (Space Shuttle main engine)*, NASA MSFC Contract NAS8-34505, Turbomachinery Laboratories Report FD-1-84 (30 January 1984)

[4] F. Dinca and C. Teodosiu, *Nonlinear and random vibrations*, Academic Press, 1973

[5] P. K. Gupta, L. W. Winn, and D. B. Wilcock, *Vibrational characteristics of ball bearings*, Trans. ASME J. of Lubrication Technology, **99F**, No. 2, 284–289 (1977)

[6] H. H. Jeffcott, *The lateral vibration of loaded shafts in the neighborhood of a whirling speed—The effect of want of balance*, Philos. Mag., Series 6, **37**, 304 (1919)

[7] M. Kubicek and M. Marek, *Computational methods in bifurcation theory and dissipative structures*, Springer-Verlag, 1983.

[8] A. H. Nayfeh, *Perturbation methods*, John Wiley & Sons, 1973

[9] T. T. Yamamoto, *On critical speeds of a shaft*, Mem. Fac. Engrg. Nagoya Univ., **6**, No. 2, (1954)